Journal of Alloys and Compounds 509 (2011) 409–413

Contents lists available at ScienceDirect

Journal of Alloys and Compounds

journal homepage: www.elsevier.com/locate/jallcom

Enhancement of upconversion luminescence of Y_2O_3:Er^{3+} nanocrystals by codoping Li^+–Zn^{2+}

Huijuan Liang[a], Yangdong Zheng[a], Guanying Chen[a], Li Wu[a], Zhiguo Zhang[a,*], Wenwu Cao[b,*]

[a] Department of Physics, Harbin Institute of Technology, 150001 Harbin, People's Republic of China
[b] Materials Research Institute, Pennsylvania State University, University Park, 16802 PA, USA

ARTICLE INFO

Article history:
Received 14 May 2010
Received in revised form 8 September 2010
Accepted 8 September 2010
Available online 17 September 2010

Keywords:
Upconversion
Nanocrystals
Rare earth
Y_2O_3

ABSTRACT

The upconversion (UC) luminescence in sol–gel synthesized Li^+, Zn^{2+}, or Li^+–Zn^{2+} codoped Y_2O_3:Er^{3+} nanocrystals were investigated under the excitation of a 970 nm diode laser. Compared to undoped Y_2O_3:Er^{3+} samples, proper doping of Li^+–Zn^{2+} leads to an drastic increase of the UC luminescence centered at 560 nm by a factor of 28. The UC luminescence enhancement is a result of the increased lifetime of the intermediate state $^4I_{11/2}$ (Er). The intensity ratio of the green over red emissions (green/red) is also affected by the codoping of Zn^{2+}, Li^+ and Li^+–Zn^{2+} ions. Our results demonstrated that the Li^+–Zn^{2+} codoping in Y_2O_3:Er^{3+} phosphors produced remarkable enhancement of the UC luminescence and green/red ratio, making this nanocrystal a promising candidate for photonic and biological applications.

1. Introduction

There has been a great interest in applying rare earth ions doped nanocrystals in the fields of photonics, biology, medicine, etc. [1–3] due to the trivalent rare earth elements with ladder-like energy levels have the ability to absorb the near-infrared (NIR) light from inexpensive NIR diode lasers and convert it into visible light [4,5]. Compared with organic fluorophores and semiconductor quantum dots, these UC nanocrystals have two important features as fluorescence labels, i.e. remarkable light penetration depth and the absence of back ground fluorescence [6,7]. Recently, biocompatible UC nanocrystals have been developed for *in vitro* imaging [8,9]. Furthermore, these UC nanocrystals may be used in multicolor imaging, which is considered an important technique for targeting and imaging of cells. However, under NIR excitation, nanocrystals usually emit several UC bands simultaneously. Therefore, designing monochromatic UC emissions with high main band and low impurity band is important [10]. In addition, insufficient intensity of the UC luminescence still constitutes the main obstacle for practical applications of these UC nanocrystals. Therefore, realization of efficient and monochromatic UC emission will have great impact in the practical application of UC nanoparticles [11–13].

Er^{3+} ions is the most studied ion in the field of upconversion materials, because it has favorable energy level structures and strong UC emissions [12–14]. Among inorganic host, Y_2O_3 exhibits higher mechanical, thermal, and chemical stability and constitutes a good candidate for biomedical and photonic applications [2,15,16]. In this study, Y_2O_3:Er^{3+} nanocrystals were chosen to accomplish high intensity and monochromatic green UC luminescence. Under the excitation of a 970 nm diode laser, the dominant UC luminescence of Y_2O_3:Er^{3+} nanocrystals are green and red UC emissions. Recently, it was found that codoping Li^+ ions can enhance UC emission and increase the intensity ratio of the green over red emissions (green/red) of Er^{3+} doped oxides [12–13,17,18].

In this paper, we report a drastic increase of the monochromaticity and great enhancement of the UC luminescence of Y_2O_3:Er^{3+} nanocrystals under a 970 nm diode laser excitation by codoping of Zn^{2+}, Li^+ or Zn^{2+} and Li^+ ions. The XRD pattern and FTIR analysis were used to characterize the crystal structures of synthesized nanocrystals. The measured lifetimes and the steady state equations were used to explain the enhancement mechanism of the observed UC emissions.

2. Experimental procedures

Nanocrystals of Y_2O_3: 0.2 mol% Er^{3+} codoped with different concentrations of Zn^{2+} (0.0, 0.5, 1, 2.5, 5.0 and 10.0 mol%), Li^+ (0.0, 0.2, 0.5, 1.0, 3.0, 5.0 and 7.0 mol%), and 2.5 mol% Zn^{2+} + 5 mol% Li^+, respectively, were synthesized by a complex procedure reported earlier [10] with a small variation by adding appropriate zinc nitrate or lithium nitrate when adding yttrium nitrate.

The synthesized powders were pressed into smooth and flat disks to be used for spectral studies. A focused 200 mW power-controllable 970 nm diode laser (Hi-Tech Optoelectronics Co. Ltd., Beijing) was used to irradiate the sample surface with the focus area of about 1 mm^2. The emitted UC fluorescence was collected by a lens-coupled monochromator (Zolix Instruments Co. Ltd., Beijing) with an attached

* Corresponding author.
E-mail addresses: zhangzhiguo@hit.edu.cn (Z. Zhang), dzk@psu.edu (W. Cao).

0925-8388/$ – see front matter © 2010 Elsevier B.V. All rights reserved.
doi:10.1016/j.jallcom.2010.09.044

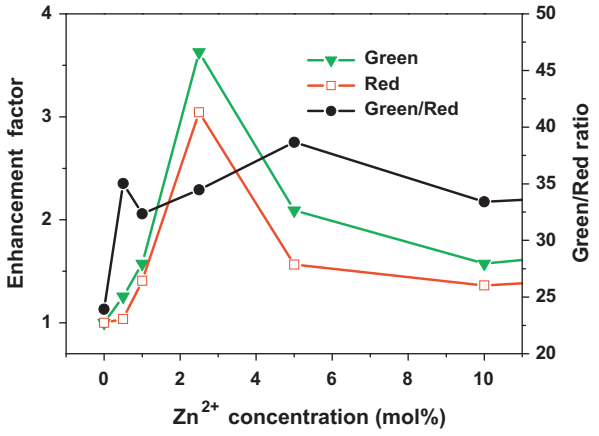

Fig. 1. Enhancement factors of the green emission, red emission and green/red ratio in Zn^{2+} doped Y_2O_3: 0.2mol% Er^{3+} nanocrystals as a function of the Zn^{2+} concentration excited by a 970 nm diode laser. (For interpretation of references to colour in this figure legend, the reader is referred to the web version of this article.)

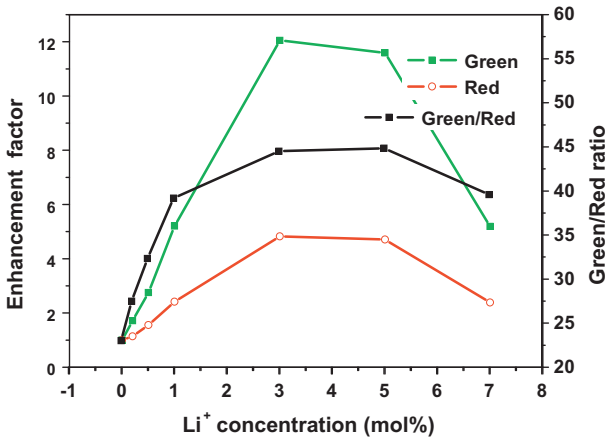

Fig. 2. Enhancement factors of the green emission, red emission and green/red ratio in Li^+ doped Y_2O_3: 0.2 mol% Er^{3+} nanocrystals as a function of Li^+ ion concentration excited by a 970 nm diode laser. (For interpretation of references to colour in this figure legend, the reader is referred to the web version of this article.)

photomultiplier tube. All spectral measurements were performed at room temperature. Time-resolved fluorescence spectra were measured as follows: a modulated square-wave electric current was input to the 970 nm diode laser to generate the NIR light beam, the fluorescence signals from the sample was detected by a NIR sensitive InGaAs photodiode (Thorlabs, DET410/M) and recorded by a Tektronic TDS 5052 digital oscilloscope with a lock-in preamplifier (Stanford Research System Model SR830 DSP) at a chopping rate of 3000 rps.

Powder X-ray diffraction (XRD) analysis was carried out using a Rigaku D/Max-2550/pc diffractometer (Cu Kα radiation) and the morphology of the powders was characterized by a HITACHI H-8100 transmission electron microscope (TEM). The Fourier transform of the infrared (FTIR) spectra were obtained using a Varian 3100 FTIR spectrometer via the potassium bromide (KBr) pellet technique, in which 1 mg of the sample was diluted by approximately 100 mg KBr powder.

3. Results and discussion

3.1. Comparison of UC luminescence

Under the excitation of a 970 nm diode laser, the UC emissions of Y_2O_3: 0.2 mol% Er^{3+} nanocrystals, codoped with 0.0, 0.5, 1, 2.5, 5 and 10 mol% Zn^{2+} ions, have been measured. The luminescence bands centered at 560-nm and 650-nm correspond to the radiations of $^2H_{11/2}/^4S_{3/2} \rightarrow {}^4I_{15/2}$ and $^4F_{9/2} \rightarrow {}^4I_{15/2}$ of Er^{3+} ions, respectively [12–14]. The UC emission is almost monochromatic green because the low concentration of Er^{3+} ions [16]. Fig. 1 shows the quantitative enhancement of the green and red emissions, and the green/red ratio as a function of Zn^{2+} concentration. The integrated intensity of green and red emissions increases sharply with Zn^{2+} ions from 0.0 to 2.5 mol%, and then increases slightly from 2.5 to 10.0 mol% compared to that of the undoped samples. The intensity of the green UC luminescence of Y_2O_3: 0.2 mol% Er^{3+} codoped with 2.5 mol% Zn^{2+} has been enhanced about 3 times compared to that of the undoped samples, and the green/red ratio is changed from 23 to 34. We observed that Zn^{2+} ions play a different role compared to a few other doping elements as doping with Mg^{2+} and Al^{3+} did not produce any enhancement in the upconversion spectrum.

A recent literature reported that codoping 5 mol% Li^+ ions in Y_2O_3:1 mol% Er^{3+} nanocrystals can enhance the UC emissions [12]. We have also verified this result. The UC emissions of Y_2O_3:0.2 mol% Er^{3+} nanocrystals codoped with 0.0, 0.2, 0.5, 1.0, 3.0, 5.0 and 7.0 mol% Li^+, respectively, have been measured under the excitation of a 970 nm diode laser. The enhancements of green and red emission, together with the green/red ratio as a function of Li^+ concentration are presented in Fig. 2. The intensity of green emission increases by a factor of 12 when the Li^+ concentration changes from 0.0 to 5.0 mol%. At higher Li^+ concentration, the enhancement

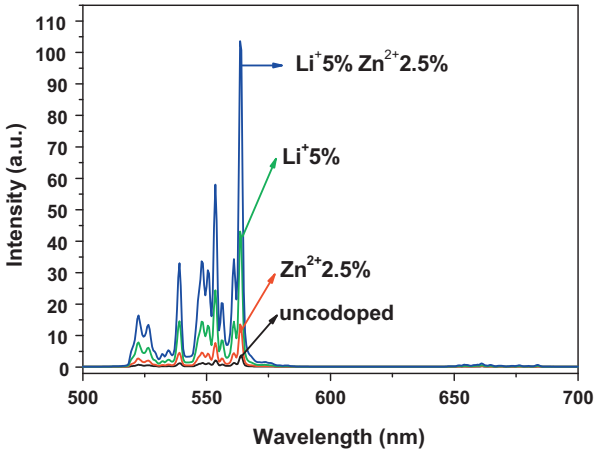

Fig. 3. Measured UC emissions in Y_2O_3: 0.2 mol% Er^{3+} nanocrystals without doping, and doped with 2.5 mol% Zn^{2+} ions, 5 mol% Li^+ ions, and 2.5 mol% Zn^{2+} +5 mol% Li^+ ions, respectively, under a 970 nm diode laser excitation.

showed slight decrease compared to the case with 5.0 mol% Li^+ ions. The green/red ratio changes from 23 to 45, then back down to 40 when the concentration of Li^+ ions changes from 0.0 to 5.0 mol%, then to 7.0 mol%.

Fig. 3 shows the UC emissions of Y_2O_3: 0.2 mol% Er^{3+} nanocrystals without codoping, codoped with 2.5 mol% Zn^{2+}, 5 mol% Li^+, and 2.5 mol% Zn^{2+} + 5 mol% Li^+ ions, respectively, under the excitation of a 970 nm diode laser. The quantitative UC luminescence enhancement and the green/red ratio of these four samples are shown in Table 1. As shown in the table, the intensities of the UC emissions are enhanced greatly with the Li^+–Zn^{2+} codoping: the green UC

Table 1
Experimental observed enhancement factor of the green UC emissions, the green/red ratio, calculated parameter β_{green}, measured lifetimes of state $^4I_{11/2}$ (Er) in Y_2O_3:0.2 mol% Er^{3+} nanocrystals without doping, doped with 2.5 mol% Zn^{2+} ions, 5 mol% Li^+ ions, and 2.5 mol% Zn^{2+} + 5 mol% Li^+ ions, respectively.

	Uncodoped	Zn^{2+}2.5%	Li^+5%	Li^+5% Zn^{2+}2.5%
Enhancement factor of the green emission	1	3.6	11	28
Green/red ratio	3	34	44	62
β_{green}	0.95	0.97	0.97	0.98
Lifetime of $^4I_{11/2}$ (ms)	0.8 (2)	1.2 (2)	2.2 (2)	2.4 (2)

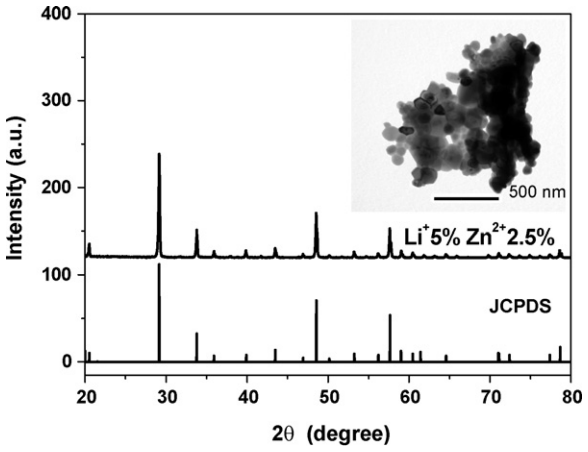

Fig. 4. Measured XRD spectra of Y_2O_3: 0.2 mol% Er^{3+} codoped with 2.5 mol% Zn^{2+} + 5 mol% Li^+ ions, contrasted with the standard pattern of JCPDS 05-0574. The inset shows its TEM image.

luminescence is enhanced by a factor of 28 and the green/red ratio is increased from 23 to 62.

3.2. Property characterization

Fig. 4 shows the XRD pattern of the Y_2O_3: 0.2 mol% Er^{3+} 2.5 mol% Zn^{2+} + 5 mol% Li^+ nanocrystals. The nanocrystals are still in cubic phase, and the XRD pattern matches well to the standard pattern of Y_2O_3 (JCPDS 89-5592). This can be understood because both Li^+ and Zn^{2+} can easily get into the host lattice owing to their small ionic radii [12,17]. So the main crystal phase of Y_2O_3 has not been affected. The inset of Fig. 4 shows a TEM micrograph of Y_2O_3 nanocrystals doped with 0.2 mol% Er^{3+}, 2.5 mol% Zn^{2+} + 5 mol% Li^+. One can see that the Y_2O_3 nanocrystals have nearly spherical shape with an average diameter of about 50 nm. The nanocrystals doped with Li^+ ions have similar morphology [17].

Fig. 5 shows the FTIR transmission spectra of Y_2O_3: 0.2mol% Er^{3+} nanocrystals without codoping, codoped with 2.5 mol% Zn^{2+}, 5 mol% Li^+ and 2.5 mol% Zn^{2+} + 5.0 mol% Li^+. The inset shows the magnified FTIR spectra in the range of 500–700 cm^{-1}. As shown in the figure, the absorption bands of OH (around 3400 cm^{-1}) become weaker with the doping of Zn^{2+}, Li^+ or Li^+–Zn^{2+} ions.

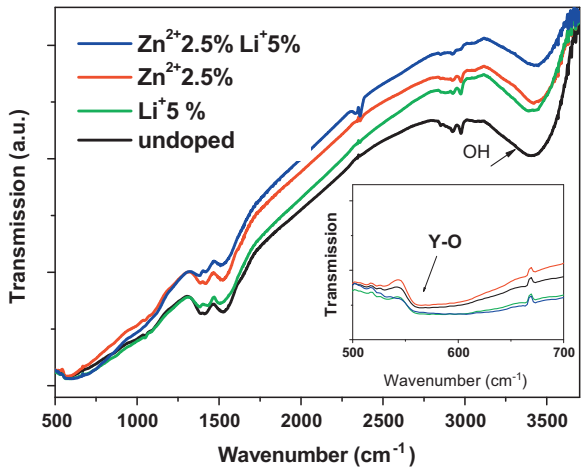

Fig. 5. Measured FTIR transmission spectra of Y_2O_3: 0.2 mol% Er^{3+} nanocrystals without codoping, and codoped with 5 mol% Li^+ ions, 2.5 mol% Zn^{2+} ions, and 2.5 mol% Zn^{2+} + 5 mol% Li^+ ions, respectively. The inset shows the magnified FIIR in the range of 500–700 cm^{-1}

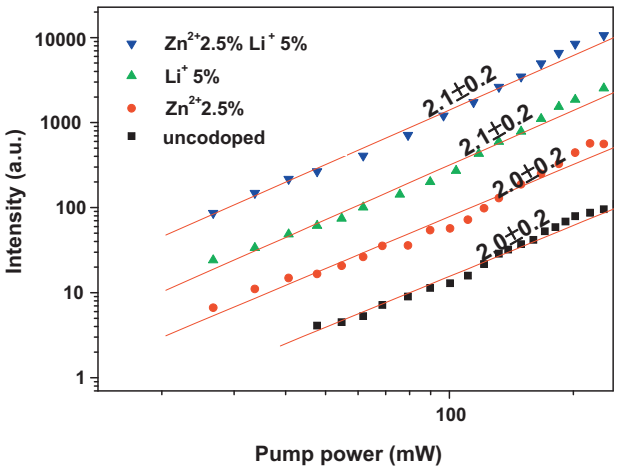

Fig. 6. Pump power dependence of the fluorescent bands centered at 564 nm in Y_2O_3: 0.2 mol% Er^{3+} nanocrystals without codoping and codoped with 2.5 mol% Zn^{2+} ions, 5 mol% Li^+ ions, and 2.5 mol% Zn^{2+}+5 mol% Li^+ ions, respectively.

The UC efficiency is regulated by nonradiative processes, which are dependent on the highest phonon energy in the materials (phonon cutoff energy and defects on the surface). The lower phonon cutoff energy can increase the UC emission by hindering nonradiative relaxations, for instance, fluorides are more UC luminescent than oxides due to their lower phonon cutoff energy. As shown in the inset of Fig. 5, the absorption band at 550 cm^{-1}, which corresponds to the vibration mode of Y–O bond, agrees well with the reported phonon cutoff energy [12]. The Y–O absorption band does not change with the Zn^{2+}, Li^+ or Li^+–Zn^{2+} codoping, which indicated that the phonon cutoff energy has not been affected by the doping of Zn^{2+} or Li^+–Zn^{2+} ions [18]. Here, codoping of Zn^{2+}, Li^+ or Li^+–Zn^{2+} ions can reduce the defects (OH group) of the nanocrystals, which help to increase the UC luminescence through hindering nanoradiative relaxations [19].

3.3. Theoretical description

In order to investigate the mechanism of UC enhancement, pump power dependence of the green emissions in Y_2O_3:0.2 mol% Er^{3+}, Y_2O_3:0.2 mol% Er^{3+}2.5 mol% Zn^{2+}, Y_2O_3:0.2 mol% Er^{3+}5 mol% Li^+ and Y_2O_3:0.2 mol% Er^{3+}2.5 mol% Zn^{2+} + 5 mol% Li^+ nanocrystals have been measured as shown in Fig. 6. The number of photons necessary to populate the upper emitting state can be obtained by the relation $I_f P^n$, where I_f is the fluorescent intensity, P is the pump laser power, and n is the number of photons required to produce the emission (at the lower pump intensity) [20,21]. As illustrated in Fig. 6, all the measured n values of the green band were about 2. This result indicates that two photon processes are involved to populate the $^2H^{<}_{11/2}/^4S_{3/2}$ state, in a good agreement with previously published data [12–14]. These experimental results in Fig. 6 indicate that the mechanism for green UC radiations is not affected by Li^+, Zn^{2+} or Li^+–Zn^{2+} codoping.

Fig. 7 presents the energy levels of the Er^{3+} ion and the proposed UC mechanism. The ions in the ground state can absorb a laser photon, excited to the intermediate $^4I_{11/2}$ state, then to the $^4F_{7/2}$ state through the excited state absorption (ESA1) process or energy transfer upconversion (ETU1) process. Nonradiative multiphonon decay is responsible for populating the $^2H^{<}_{11/2}/^4S_{3/2}$ and $^4F_{9/2}$ states. There is another mechanism to populate the $^4F_{9/2}$ state, i.e., the Er^{3+} ion at state $^4I_{11/2}$ can nonradiatively relax to the $^4I_{13/2}$ state, then being further excited to the $^4F_{9/2}$ state by ESA2 or ETU2 processes. The cross relaxation (CR) process

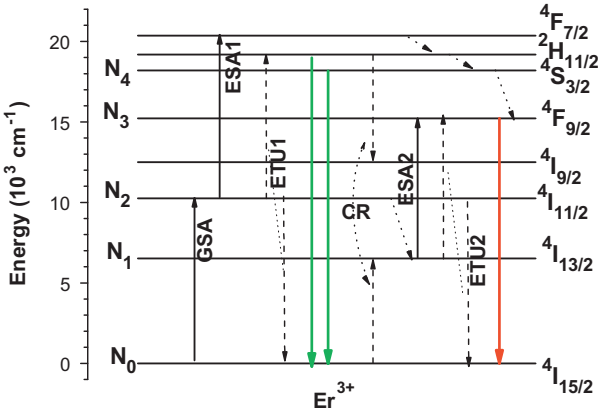

Fig. 7. Energy-level diagram of Er^{3+} ion as well as the UC mechanisms for the green and red emissions.

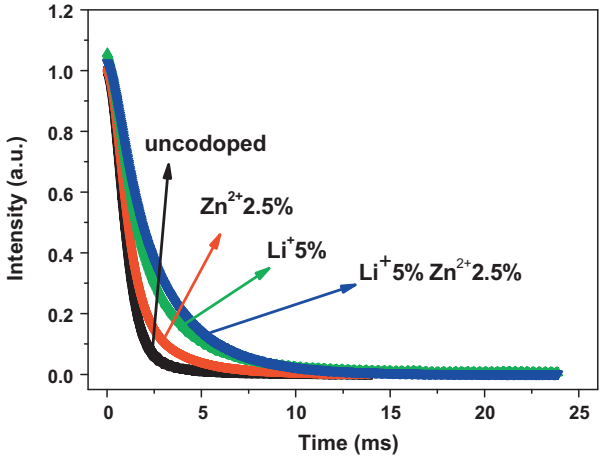

Fig. 8. Decay profiles of the transition in Y_2O_3: 0.2 mol% Er^{3+} nanocrystals without codoping and codoped with 2.5 mol% Zn^{2+} ions, 5 mol% Li^+ ions, and 2.5 mol% Zn^{2+}+5 mol% Li^+ ions, respectively.

$^2H_{11/2}(Er) + {}^4I_{15/2}(Er) \rightarrow {}^4I_{9/2}(Er) + {}^4I_{13/2}(Er)$ is also responsible for populating the $^4I_{13/2}$ state (further to the $^4F_{9/2}$ state). The efficiency of the energy transfer process (CR) would decrease on increasing the average distance between Er^{3+} ions. Therefore, when the concentration of Er^{3+} ions is lower than 0.2 mol%, the CR process $^2H_{11/2}(Er) + {}^4I_{15/2}(Er) \rightarrow {}^4I_{9/2}(Er) + {}^4I_{13/2}(Er)$ is suppressed so that the red emission is greatly reduced, and the UC emission becomes nearly monochromatic green [12,16].

Now, the effects of Li^+, Zn^{2+} or Li^+–Zn^{2+} co-doping on the change of green/red ratio can be explained. When the Zn^{2+}, Li^+ or Li^+–Zn^{2+} are codoped in the nanocrystals, the OH groups of the nanocrystals are reduced as shown in Fig. 5, which can decrease the nonradiative processes from state $^2H^{<}_{11/2}/{}^4S_{3/2}$ to state $^4F_{9/2}$ and from state $^4I_{11/2}$ to state $^4I_{13/2}$. All of these processes can reduce the population in the $^4F_{9/2}$ state, which is responsible for the red emission. Also, codoping of these no-luminescence ions can dissociate the Er^{3+} clusters in the Y_2O_3 crystal lattice, thus, hamper the red emission by avoiding the CR process [16].

In order to theoretically account for the enhancement of the UC emissions, steady-state equation is given in Eq. (1) [12], which describes the relationship between the green UC emission and the lifetime of state $^4I_{11/2}$:

$$I_{\text{green}} = \beta_{\text{green}}(\tau_2 R_1 R_2 N + C\tau_2{}^2 R_1{}^2 N^2)h\nu_{\text{green}} \quad (1)$$

where $N_i(\tau_i)$ is the population density (decay time) shown in Fig. 7; R_1 and R_2 are the rates of GSA and ESA1 processes, which are constant here due to the identical excitation condition; C is the coefficient of ETU 1 process; β_{green} is the ratio of the radiation rate to the decay rate in the $^2H^{<}_{11/2}/{}^4S_{3/2}$ state, which can be calculate by the green/red ratio. There are two hypotheses in the derivation of Eq. (1): $N \approx N_0$ and $R_2N_2 + 2CN_2^2 \ll N_2/\tau_2$, which are reasonable because the green emission is verified to be two photon processes [20,21]. It should be mentioned that the parameter β_{green} has only a small increase for 2.5 mol% Zn^{2+} or 5 mol% Li^+ doped samples, which cannot lead to great enhancement of the green UC emission, as shown in Table 1. Here the only variable is the lifetime of state $^4I_{11/2}$

Fig. 8 shows the decay profiles of state $^4I_{11/2}$ (1015 nm) of nanocrystals Y_2O_3:0.2 mol% Er^{3+}, Y_2O_3:0.2 mol% Er^{3+}2.5 mol% Zn^{2+}, Y_2O_3:0.2 mol% Er^{3+}5.0 mol% Li^+ and Y_2O_3:0.2 mol% Er^{3+} 2.5 mol% Zn^{2+}5.0 mol% Li^+ measured by square modulation of the 970 nm excitation laser. The lifetimes of state $^4I_{11/2}$(Er) of these nanocrystals were calculated using the exponential fitting and the results are shown in Table 1. The lifetimes of the intermediate $^4I_{11/2}$ state were 0.8(2), 1.2(2), 2.0(2) and 2.4 (2) ms for none doped, Zn^{2+}, Li^+, or Li^+–Zn^{2+} codoped nanocrystals, respectively. Doping Li^+ or Zn^{2+} ions can prolong the lifetime of the $^4I_{11/2}$ state, and the lifetime can be increased even longer when both Li^+ and Zn^{2+} are codoped into the nanocrystals. The prolonged lifetime may arise from the tailored local environment of the Er^{3+} ions and the reduction of the OH groups [18,19]. According to Eq. (1), the long lifetime of state $^4I_{11/2}$ can lead to strong green UC luminescence, which agrees well with the experiment result shown in Fig. 3.

It should be pointed out that the lifetime of state $^4I_{11/2}$ has been prolonged more in the Li^+ ions doped sample than the Zn^{2+} ions doped sample. We think that the longer lifetime in the Li^+ ions doped sample may result from the more severe modification of the Er^{3+} local environment. The Li^+ and Zn^{2+} ions both can get into the lattice of Y_2O_3 crystals and tailor the local environment of the Er^{3+} ions. The tailoring effect induced by Li^+ ions and induced by Zn^{2+} ions are independent, so the Li^+–Zn^{2+} codoped nanocrystals has the longest lifetime. Also, the codoping of these ions can reduce the OH groups of the nanocrystals, as shown in Fig. 5. These two factors help to prolong the lifetime of the intermediate state $^4I_{11/2}$. Since Li^+ and Zn^{2+} ions can play their roles independently and constructively, the Li^+–Zn^{2+} codoped sample have the longest intermediate lifetime.

4. Conclusions

In summary, proper amount of Zn^{2+}, Li^+ or Li^+–Zn^{2+} ions codoping can enhance the intensity of UC emissions and increase the green/red ratio. In our experiment, the intensity of UC luminescence has been enhanced by a factor of 28 through the codoping of Li^+–Zn^{2+} ions. Theoretical investigations show that the enhanced UC emissions arise from the prolonged lifetime of the intermediate state $^4I_{11/2}$. The much prolonged lifetimes are mainly induced by the tailoring of the local environment of Er^{3+} ions and the reduction of OH groups. The tailoring effect induced by Li^+ ions and Zn^{2+} ions are constructive, so that the Li^+–Zn^{2+} codoped nanocrystals have the strongest UC emissions.

Acknowledgements

The work is supported by the SIDA Asian-Swedish Research Partnership Program, the 863 Hi-Tech Research and Development Program of People's Republic of China, the Harbin City Bureau of Science and Technology Key project fund (2009AA3BS131) and the Harbin Institute of Technology through Programs for Interdisciplinary Basic Research on Science, Engineering and Medicine.

References

[1] F. Wang, X.G. Liu, Chem. Soc. Rev 38 (2009) 976.
[2] L. Xiong, T. Yang, Y. Yang, C. Xu, F. Li, Biomaterials 31 (2010) 7078.
[3] X. Qin, G. Zhou, H. Yang, Y. Yang, J. Zhang, S. Wang, J. Alloys Compd. 493 (2010) 672.
[4] F. Auzel, Chem. Rev. 104 (2004) 139.
[5] J.F. Suyver, J. Grimm, M.K van Veen, D. Biner, K.W. Kramer, H.U. Güdel, J. Lumin. 117 (2006) 1.
[6] L.X. Xiong, Z.G. Chen, Q.W. Tian, T.Y. Cao, C.J. Xu, F.Y. Li, Anal. Chem. 81 (2009) 8687.
[7] Z. Tian, G.Y. Chen, X. Li, H.J. Liang, Y.S. Li, Z.G. Zhang, Y. Tian, Laser. Med. Sci. 25 (2010) 479.
[8] M.X. Yu, F.Y. Li, Z.G. Chen, H. Hu, C. Zhan, C.H. Huang, Anal. Chem. 81 (2009) 930.
[9] J. Zhou, Y. Sun, X.X. Du, L.Q. Xiong, H. Hu, F.Y. Li, Biomaterials 31 (2010) 3287.
[10] Y.Q. Sheng, L.L. Xu, J. Liu, D. Zhai, Z.G. Zhang, J. Lumin. 130 (2010) 338.
[11] Y. Bai, Y. Wang, G. Peng, K. Yang, X. Zhang, Y. Song, J. Alloys Compd. 478 (2009) 676.
[12] G.Y. Chen, H.C. Liu, G. Somesfalean, Y.Q. Sheng, H.J. Liang, Z.G. Zhang, Q. Sun, F.P. Wang, Appl. Phys. Lett. 92 (2008) 113114.
[13] Y.F. Bai, Y.X. Wang, K. Yang, X.R. Zhang, G.Y. Peng, Y.L. Song, J. Phys. Chem. C 112 (2008) 12259.
[14] L. Lin, G. Ren, M. Chen, Y. Liu, J. Alloys Compd. 486 (2009) 261.
[15] Q. Lü, Y. Wu, L. Ding, G. Zu, A. Li, Y. Zhao, H. Cui, J. Alloys Compd. 496 (2010) 488.
[16] F.J. Vetrone, C. Boyer, J.A. Capobianco, A. Speghini, M. Bettinelli, Chem. Mater. 15 (2003) 2737.
[17] H.J. Liang, G.Y. Chen, H.C. Liu, Z.G. Zhang, J. Lumin. 129 (2009) 197.
[18] G Chen, H. Liu, H. Liang, G. Somesfalean, Z. Zhang, J. Phys. Chem. C 112 (2008) 12030.
[19] Y.F. Bai, K. Yang, Y.X. Wang, X.R. Zhang, Y.L. Song, Opt. Commun. 281 (2008) 2930.
[20] J.F. Suyver, A. Aebischer, S. Garcia-Revilla, P. Güdel, H.U. Gerner, Phys. Rev. B 71 (2005) 125123.
[21] G.M. Pollnau, D.R. Gamelin, S.R. Lüthi, H.U. Güdel, Phys. Rev. B 61 (2000) 3337.